Contents lists available at ScienceDirect

Chinese Journal of Physics

journal homepage: www.sciencedirect.com/journal/chinese-journal-of-physics

Numerical simulations of combined effect of viscosity variation and magnetohydrodynamic (MHD) characteristics for wide porous slider bearings with exponential film profile

Zahoor Iqbal [a,*], Nisha A. [e], Vinoth kumar B. [e], Huiying Xu [a,*], Xinzhong Zhu [a,b,c,d,*], Ridha Selmi [f,*], Sahar Ahmed Idris [g], Ines Hilali Jaghdam [h], Ahmed M. Abed [i,j]

[a] *School of Computer Science and Technology (School of Artificial Intelligence), Zhejiang Normal University, Jinhua 321004, PR China*
[b] *Research Institute of Hangzhou Artificial Intelligence, Zhejiang Normal University, Hangzhou, 311231, PR China*
[c] *College of Computer Science and Artificial Intelligence, Wenzhou University, Wenzhou 325035, PR China*
[d] *Zhejiang Key Laboratory of Intelligent Education Technology and Application, Zhejiang Normal University, Jinhua, 321004, Zhejiang, PR China*
[e] *Department of Mathematics, Rajalakshmi Institute of Technology (RIT), Poonamalle, Chennai 600124, Tamil Nadu, India*
[f] *Department of Mathematics, College of Science, Northern Border University, Arar, Saudi Arabia*
[g] *Faculty of Engineering, Department of Industrial Engineering, King Khalid University, Abha, Saudi Arabia*
[h] *Department of Computer Science and Information Technology, Applied College, Princess Nourah bint Abdulrahman University, P.O. Box 84428, Riyadh 11671, Saudi Arabia*
[i] *Industrial Engineering Department, Engineering College, Prince Sattam bin Abdulaziz University, Al-Kharj 16273, Saudi Arabia*
[i] *Department of Industrial Engineering, Zagazig University, Zagazig 44519, Egypt*

A R T I C L E I N F O

Keywords:
Numerical simulations
Hartmann number
Pressure
Load carrying capacity
Porous Slider Bearings
Mining industry

A B S T R A C T

The theory of magneto hydrodynamic (MHD) thin film lubrication is applied to numerically analyze the MHD properties (including steady film pressure, non-dimensional load capacity, non-dimensional stiffness coefficient, and non-dimensional damping coefficient) of wide-exponential shaped porous slider bearings containing an electrically conducting fluid under the influence of a transverse magnetic field. The MHD dynamic Reynolds-type equation, which incorporates transient squeezing motion, is produced by merging the continuity equation with the MHD motion equations. A closed-form solution is utilized to determine the static film pressure. Moreover, MATLAB (r2018b) numerical simulations are performed to see the effects of distinct parameters on velocity and pressure distributions. The findings suggest that the presence of externally applied magnetic fields indicates an increase in film pressure. The influence of an applied magnetic field on the lubricant flow is analyzed, considering viscosity variations due to temperature and pressure changes. The governing equations are formulated and solved to determine the pressure distribution, load-carrying capacity, and frictional characteristics. The results reveal that the MHD effect enhances the bearing's load capacity, while viscosity variation significantly influences lubricant behavior, leading to optimized performance. The findings provide insights into

* Corresponding authors.
E-mail addresses: izahoor@math.qau.edu.pk, izahoor@zjnu.edu.cn (Z. Iqbal), xhy@zjnu.edu.cn (H. Xu), zxz@zjnu.edu.cn (X. Zhu), Ridha.Selmi@nbu.edu.sa (R. Selmi).

https://doi.org/10.1016/j.cjph.2025.03.037
Received 11 February 2025; Received in revised form 24 March 2025; Accepted 24 March 2025

improving bearing efficiency in high-temperature, electrically conductive fluid applications, thermal engineering, mining industry, and energy sector.

The influence of the applied magnetic field, as shown by the Hartmann number, greatly enhances the load-bearing capacity when contrasted with the non-conducting lubricant (NCL) scenario values. Moreover, with increasing Hartmann number, these improvements in bearing MHD characteristics become increasingly obvious and decreasing minimum film thickness.

1. Introduction

The hydrodynamic lubrication characteristics have typically been examined under the premise that a lubricant behaves as either a Newtonian or a non-Newtonian fluid, with the viscous fluid following the principles of classical continuum theory. Initially, Stoke (1966) formulated several micro continuum theories to characterize the behavior of non-Newtonian fluids containing microstructure. Stoke's micro continuum theory of fluids represents the simplest modification and advancement of the classical continuum theory of fluid, accommodating polar effects such as anti-symmetric stress tensors and couple stress body couples. Magneto hydrodynamic is concerned with the physical system specified by the equation that result from the fusion of those hydrodynamic and electromagnetic theory. A magnetic field which is generated by the induced current is added to the applied magnetic field. MHD is interesting from several standpoints. Magneto-fluids can carry current which means that they can both generate field and can be influenced by magnetic fields. Bernard and Hamerock [1] initially explored the properties of fluid film lubrication. A systematic investigation of magneto hydrodynamics was initiated by Alfven Reddy and colleagues [2] examined the joint effect of changes in viscosity and squeeze behavior on the performance of narrow hydrodynamic journal bearings utilizing a couple stress fluid model. A number of researchers investigated the MHD properties using couple stress as a lubricant.

Naduvinamani *et al.* [4] explored the MHD lubrication of a couple stress squeeze film on circular stepped plates, while Hanumagowda *et al.* [3] examined the impact of MHD with couple stress on a plane slider bearing. Naduvinamani *et al.* [6] investigated the MHD influence on an exponential film configuration using a pair stress fluid, while Lin [5] analyzed the MHD dynamic characteristics of a broad slider bearing with a power law film profile. Roughness denotes the irregularity or uneven quality of a texture and stands as one of the primary surface topographic descriptions. It illustrates the surface's smoothness at a specific length scale. Consequently, roughness standards are essential in areas such as brake pads, flooring, and tires. The influence of roughness parameters on lubrication regarding topics such as sliding surface lubrication, compliant surfaces, and roller bearing wear has also been investigated.

Numerous specialists have investigated different types of bearings with the roughness effect. While Kudenatti *et al.* [8] considered the MHD squeeze film between porous, rough rectangular plates and provided a numerical solution for it, Kesavan *et al.* [7] investigated the MHD porous parallel rectangular plates with a finite number of pores with a roughness effect.

Surface roughness and MHD effect between two finite rectangular plates were given by Bujurke [9]. Christensen [10] presents a stochastic model for hydrodynamic lubrication of uneven surfaces.

Slider bearings are those that generate solely sliding friction. The shaft is supported in most cases by the sliding surface, with oil and air in between to aid sliding movement. Porous sliding bearings are very useful in mining industry, mechanical engineering and many other thermal engineering applications. In mining industry, the porous sliding bearings can be used for enhanced load bearing in crushers and mills, for improving the performance in drilling equipment and enhanced thermal stability. The MHD effects and porous bearing structures work together to enhance heat dissipation, maintain ideal operating temperatures, and avoid overheating, all of which are critical in the mining sector and for the thermal progress of electronics.

The slider bearing featuring an exponential profile for various lubricants has been examined in many studies. The impact of porous exponential slider bearings on MHD pair stress was studied by Hanumagouda *et al.* [11]. Lin *et al.* [12] examined the dynamic characteristics of wide slider bearings featuring exponential film profiles.

The dynamic characteristics of an exponential slider bearing with MHD couple stress were examined by Naduvinamani *et al.* [13]. For various film profiles, Biradar *et al.* [14] and Sreekala *et al.* [15] investigated the couple stress effect on slider bearings.

The combined effects of surface roughness and viscosity variation on the couple stress squeeze film properties of short journal bearings are theoretically analyzed and presented. The Christensen stochastic theory is used to mathematically derive the modified stochastic Reynold's equation that takes into account the fluid's viscosity variation of couple stresses and the randomized surface roughness structure on the bearing surface. By analyzing how viscosity variations influence the behavior of MHD-based lubrication, this study helps optimize the design and performance of slider bearings under different operating conditions, ensuring efficient load-carrying capacity and reduced friction. Here we have used MATLAB (R2018b) to solve the equations numerically. The problem has not been encountered earlier by any other author. By improving lubrication efficiency and reducing energy losses due to friction and wear, this study contributes to the development of more energy-efficient and sustainable mechanical systems.

Overall, this study bridges the gap between theoretical fluid dynamics, magnetic field applications, and practical engineering solutions, making it highly valuable for both researchers and engineers involved in bearing technology and lubrication science.

Research Questions:

- How does the variation in lubricant viscosity influence the pressure distribution and load-carrying capacity of wide porous slider bearings with an exponential film profile?

- What is the impact of temperature-dependent viscosity changes on the lubrication performance of porous slider bearings under different operating conditions?
- What is the role of MHD effects in controlling the flow behavior of conducting lubricants within a porous bearing system?

Viscosity represents internal friction of the fluid, such internal forces in flowing fluid result from cohesion and molecule.

2. Mathematical formulations

The physical geometry of a wide porous slider bearing with a length L and a sliding velocity U in the x-direction and a squeezing velocity $\frac{\partial h}{\partial t}$ in the z-direction is shown in Fig. 1. The exponential film thickness is calculated as follows

$$h(x,t) = e^{-x\frac{(\ln r)}{L}} h_m(t). \tag{1}$$

Here '$h_m(t)$' denotes the minimum film thickness at outlet '$r = \frac{d+h_m(t)}{h_m(t)}$' and inlet-outlet film ratio, where 'd' is the shoulder height representing the difference between the height of the inlet and the height of the outflow.

Assumptions

- In contrast to viscous forces, inertial forces are regarded as insignificant.
- Fluid film is considered as thin.
- The body forces and body couples are considered insignificant.
- An electrically conductive immiscible isothermal fluid with electrical properties is supposed to be the lubricant.
- In the z-direction, there is an externally uniform transverse magnetic field.
- The lubricant is considered a Newtonian, incompressible fluid with viscosity varying as a function of temperature and pressure.
- The lubrication film thickness is small compared to the bearing length, allowing the use of the Reynolds equation under the thin film assumption.
- The fluid flow within the lubrication film is assumed to be in a steady-state condition, with no transient effects.
- The lubricant flow is assumed to be laminar, as the Reynolds number is low due to the small film thickness and moderate sliding velocities.

The governing equation is given by

$$\frac{\partial u}{\partial x} + \frac{\partial w}{\partial z} = 0, \tag{2}$$

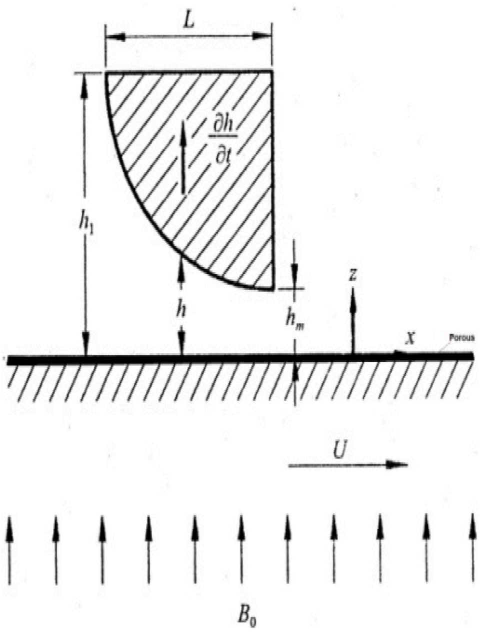

Fig. 1. Physical Representation of the Problem.

$$\frac{\partial p}{\partial x}=\mu\frac{\partial^2 u}{\partial z^2}-\sigma B_0\left(E_y+uB_0\right), \tag{3}$$

$$\frac{\partial p}{\partial z}=0. \tag{4}$$

The no slip condition for the boundary at porous bearing surfaces are

$$u=U \text{ and } w=0 \text{ at } z=0. \tag{5}$$

$$u=0 \text{ and } w=\frac{dh}{dt} \text{ at } z=h. \tag{6}$$

The solution is given by

$$u=A_1e^{\sqrt{\frac{\sigma}{\mu}}B_0z}+B_1e^{-\sqrt{\frac{\sigma}{\mu}}B_0z}-\frac{1}{\sigma{B_0}^2}\left[\frac{\partial p}{\partial x}+\sigma B_0E_y\right]. \tag{7}$$

The x-direction velocity component is provided by

$$u=U\left[\cosh\left(\frac{Mz}{h_{m_0}}\right)-\coth\left(\frac{Mz}{h_{m_0}}\right)\sinh\left(\coth\left(\frac{Mz}{h_{m_0}}\right)\right)\right]+\frac{1}{\sigma{B_0}^2}\left[\frac{\partial p}{\partial x}+\sigma B_0E_y\right]\left[\cosh\left(\frac{Mz}{h_{m_0}}\right)-1-\tanh\left(\frac{Mz}{h_{m_0}}\right)\sinh\left(\coth\left(\frac{Mz}{h_{m_0}}\right)\right)\right], \tag{8}$$

where M is the Hartmann number and signifies the constant minimum film thickness h_{m_0} at the end defined as

$$M=B_0h_{m_0}\sqrt{\frac{\sigma}{\mu}}. \tag{9}$$

In this analysis, it is assumed that the fluid has no external circuit and that the bearing surfaces are perfect insulators. The electric field is then estimated by requiring a zero net current flow.

$$\int_{z=0}^{h}\left(E_y+uB_0\right)dz=0. \tag{10}$$

Taking the continuity equation (8.2) and integrating it over the film thickness with respect to z

$$\int_{z=0}^{h}\frac{\partial u}{\partial x}dz=-\int_{z=0}^{h}\frac{\partial w}{\partial z}dz. \tag{11}$$

Performing the integration together with the boundary condition equation (8.5) and (8.6), the MHD dynamic equation is defined as

$$\frac{1}{12}\frac{\partial}{\partial x}\left[\frac{f(h,M)}{\mu}\frac{\partial p}{\partial x}\right]-\frac{1}{2}U\frac{\partial h}{\partial x}=\frac{\partial h}{\partial t}. \tag{12}$$

Since experiments have shown that the highest temperature occurs in areas with the thinnest film thickness, a viscosity-temperature correlation can actually be substituted with a viscosity-film thickness correlation. when the viscosity 'μ_1' at $h=h_1=c(1+\varepsilon)$ (inlet condition) is known, then

$$\mu=\mu_1\left(\frac{h}{h_1}\right)^Q. \tag{13}$$

In most cases, according to the nature of lubricant, the value of Q lies between 0 and 1. The exponent 'Q' can be calculated using the following formula.

$$Q=\frac{\log\left(\frac{\mu_1}{\mu_2}\right)}{\log\left(\frac{h_1}{h_2}\right)}, \tag{14}$$

where, μ_2 is taken as the outlet viscosity with the film thickness as h_2. Also, Q $(0\le Q\le 1)$ is determined by the type of lubricant used; for ideal Newtonian fluids, $Q=0$; for perfect gases, $Q=1$.

The updated Reynold's equation thus becomes

$$\frac{\partial}{\partial x}\left[\frac{f(h,M)}{\mu_1}\frac{\partial p}{\partial x}\left(\frac{h_1}{h}\right)^Q\right]=6U\frac{\partial h}{\partial x}+12\frac{\partial h}{\partial t}, \tag{15}$$

$$\text{where } f(h,M) = 6h_{m_0}\frac{h}{M^2}\left[\frac{Mz}{h_{m_0}}\coth\left(\frac{1}{2}\frac{Mz}{h_{m_0}}\right) - 2\right], \tag{16}$$

$$h(x,t) = h_m(t)e^{-x\ln r}, \tag{17}$$

$$\text{where } r = \frac{d + h_m(t)}{h_m(t)}, \tag{18}$$

$$h_m(t) = 1 + \varepsilon, \varepsilon \leq\leq 1, \tag{19}$$

$$H = \overline{h}(t) + h_s(x,y). \tag{20}$$

The first part '$\overline{h}(t)$' is the nominal portion of the film, '$h_s(x,y)$' is defined as x and y random function having mean equal to zero.

2.1. Stochastic Reynold's equation

Let $h_s(x,y)$ be the stochastic film thickness probability derivative function defined as $f(h_s)$. Taking the average of the stochastic Eqs. (15)

$$\frac{\partial}{\partial x}\left[\frac{E(f(h,M))}{\mu_1}\frac{\partial E(p)}{\partial x}\left(\frac{h_1}{h}\right)^Q\right] = 6U\frac{\partial E(h)}{\partial x} + 12\frac{\partial E(h)}{\partial t}, \tag{21}$$

$$\text{where } E(.) = \int_{-\infty}^{\infty}(.)f(h_s)dh_s, \tag{22}$$

$$\text{where } \alpha = E(h_s), \tag{23}$$

$$\sigma^2 = E(h_s - \alpha)^2, \tag{24}$$

$$\varepsilon = E(h_s - \alpha)^3. \tag{25}$$

The mean value is given by α. The symmetry of the variables is measured by ε.

For the probability function defined by Christensen, it is assumed that

$$f(h_s) = \left\{\begin{array}{c}\frac{35}{32c^7}\left[\left(c^2 - {h_s}^2\right)^3\right], -c < h_s < c \\ 0 \text{ elsewhere}\end{array}\right\}, \tag{26}$$

where '$\sigma = c/3$' is the standard deviation.

$$E(H) = \int_{-c}^{c} Hf(h_s)ds, \tag{27}$$

$$= \int_{-c}^{c}(h + h_s)f(h_s)ds, \tag{28}$$

$$= \int_{-c}^{c}(h)\frac{35}{32c^7}\left(c^2 - {h_s}^2\right)^3dh_s\int_{-c}^{c}(h_s)\frac{35}{32c^7}\left(c^2 - {h_s}^2\right)^3dh_s, \tag{29}$$

$$= h(t), \tag{30}$$

$$\text{where } \int_{-c}^{c}\frac{35}{32c^7}\left(c^2 - {h_s}^2\right)^3dh_s = 1. \tag{31}$$

2.2. Transverse roughness

The film thickness takes the shape of a one-dimensional transverse roughness pattern composed of long thin ridges and valleys running perpendicular to the sliding surface (z-direction).

$$H = h(x,t) + h_s. \tag{32}$$

The Reynold's Eq. (31) thus assumes the following form.

$$\frac{\partial}{\partial x}\left[\frac{1}{E\left[\frac{1}{(f(h,M))}\right]}\frac{{h_1}^Q}{h^Q}\frac{\partial E(p)}{\partial x}\right] = 6U\frac{\partial}{\partial x}\left[\frac{E\left(\frac{1}{h^2}\right)}{E\left(\frac{1}{h^3}\right)}\right] + 12\frac{\partial E(H)}{\partial t}. \tag{33}$$

The modified stochastic MHD couple stress Reynold's equation for both types of roughness patterns is obtained by combining the equations (8.35) and (8.53). where,

$$G(h,M,c) = \left\{\begin{array}{l} E(f(h,M))\ \text{'For longitudinal roughness'} \\ E\left(\dfrac{1}{f(h,M)}\right)\ \text{'For transverse roughness'}\end{array}\right\}, \tag{34}$$

$$\chi(h,c) = \left\{\begin{array}{l} E(h)\ \text{'For longitudinal roughness'} \\ E\left(\dfrac{1}{h^2}\right)\ \text{'For transverse roughness'}\end{array}\right\}, \tag{35}$$

$$\text{and}\, E(f(h,M)) = \frac{35}{32c^7}\left[\int_{-c}^{c} f(h,M)\left(c^2 - {h_s}^2\right)^3 dh_s\right], \tag{36}$$

$$E\left(f(h,M)^{-1}\right) = \frac{35}{32c^7}\int_{-c}^{c}\left[\frac{\left(c^2 - {h_s}^2\right)^3}{f(h,M)}\right] dh_s\,. \tag{37}$$

Then the above equation (8.53) becomes

$$\frac{\partial}{\partial x}\left[G(h,M,c)\frac{{h_1}^Q}{h^Q}\frac{\partial E(p)}{\partial x}\right] = 6U\frac{\partial(\chi(h,c))}{\partial x} + 12\frac{\partial E(H)}{\partial t}. \tag{38}$$

Incorporating the non-dimensional parameters and variables

$$x^* = \frac{x}{L}, p^* = \frac{E(p){h_0}^2}{\mu UL}, t^* = \frac{tU}{L}, l^* = \frac{l}{2}\left(\frac{1}{h_m}\right), h^* = \frac{h}{h_0}, M = B_0 h_0\sqrt{\frac{\sigma}{\mu}}, \overline{H} = \frac{H}{h_0} = \frac{h}{h_0} + \frac{h_s}{h_0} = \overline{h} + h_s, c^* = \frac{c}{h_m}\,. \tag{39}$$

The film pressure's boundary condition at $p = 0$ at $x^* = 0$ and $x^* = -3$, $E(p) = 0$ at $x^* = 0$ and $x^* = -3$ and $\frac{dE(p)}{dx} = 0$ at $x^* = 0$. Applying the following boundary conditions and integrating twice with respect x, we get

$$p^* = \left[6h_m - \frac{12}{\ln(\delta+1)}\frac{dH}{dt}\right]\int_{x^*=0}^{x^*}\frac{h_e(x)h^Q}{E(G(h,M,c)){h_1}^Q}dx^* + c_1\left(h_m,\frac{dH}{dt}\right)\int_{x^*=0}^{x^*}\frac{h^Q}{E(G(h,M,c)){h_1}^Q}dx^*, \tag{40}$$

$$\text{where}\ h_e(x) = e^{-x\ln(\delta+1)}, \tag{41}$$

$$c_1\left(h_m,\frac{dH}{dt}\right) = -\left[6h_m - \frac{12}{\ln(\delta+1)}\frac{dH}{dt}\right]\frac{\displaystyle\int_{x^*=0}^{3}\frac{h_e(x)}{E(G(h,M,c))}dx^*}{\displaystyle\int_{x^*=0}^{3}\frac{1}{E(G(h,M,c))}dx^*}. \tag{42}$$

The non-dimensional formula for film force is found by integrating Eq. (40) over the film region, and it is given by

$$F = \int_{x^*=0}^{-3} p^* dx^*, \tag{43}$$

$$F = \left[6h_m - \frac{12}{\ln(\delta+1)}\frac{dH}{dt}\right]\int_{x^*=0}^{1}\int_{x^*=0}^{x^*}\frac{h_e(x)h^Q}{E(G(h,M,c)){h_1}^Q}dx^*dx^* + c_1\left(h_m,\frac{dH}{dt}\right)\int_{x^*=0}^{1}\int_{x^*=0}^{x^*}\frac{h^Q}{E(G(h,M,c)){h_1}^Q}dx^*dx^*, \tag{44}$$

$$c_1\left(h_m,\frac{dH}{dt}\right)=-\left[6h_m-\frac{12}{\ln(\delta+1)}\frac{dH}{dt}\right]\frac{\int_{x^*=0}^{3}\frac{h_e(x)}{E(G(h,M,c))}dx^*}{\int_{x^*=0}^{3}\frac{1}{E(G(h,M,c))}dx^*}. \tag{45}$$

2.3. Steady state characteristics

Both the steady film pressure and the steady load-carrying capacity can be calculated using Eqs. (40) and (44), respectively, by keeping the minimum film height constant and the squeezing velocity zero.

$$[p^*]_{\text{steadystate}}=[6h_m]\int_{x^*=0}^{x^*}\frac{h_e(x)h^Q}{E(G(h,M,c))h_1{}^Q}dx^*+c_1(h_m,V=0)\int_{x^*=0}^{x^*}\frac{h^Q}{E(G(h,M,c))h_1{}^Q}dx^*$$

$$[W^*]_{\text{steady state}}=[F]_{\text{steady state}}=[6h_m]\int_{x^*=0}^{1}\int_{x^*=0}^{x^*}\frac{h_e(x)h^Q}{E(G(h,M,c))h_1{}^Q}dx^*dx^*+c_1(h_m,V=0)\int_{x^*=0}^{1}\int_{x^*=0}^{x^*}\frac{h^Q}{E(G(h,M,c))h_1{}^Q}dx^*dx^*. \tag{46}$$

The partial derivative of film force with respect to the minimal film thickness can be used to calculate the linear dynamic stiffness coefficient.

$$\begin{gathered}S^*=-\left(\frac{\partial F}{\partial h_m}\right)=6\int_{x^*=0}^{-3}\int_{x^*=0}^{x^*}\frac{h_e(x)h^Q}{E(G(h,M,c))h_1{}^Q}dx^*dx^*+6h_m\left[\int_{x^*=0}^{-3}\int_{x^*=0}^{x^*}\frac{h_e(x)h^Q}{E(G(h,M,c))h_1{}^Q}\frac{\partial f}{\partial h_m}dx^*dx^*\right]+\\ \frac{\partial c_1}{\partial h_m}\int_{x^*=0}^{-3}\int_{x^*=0}^{x^*}\frac{h^Q}{E(G(h,M,c))h_1{}^Q}dx^*dx^*-c_1\left[\int_{x^*=0}^{-3}\int_{x^*=0}^{x^*}\frac{h^Q}{E(G(h,M,c))h_1{}^Q}\frac{\partial f}{\partial h_m}dx^*dx^*\right],\end{gathered} \tag{47}$$

$$\frac{\partial c_1}{\partial h_m}=\frac{\partial}{\partial h_m}\left[-\left[6h_m-\frac{12}{\ln(\delta+1)}V\right]\frac{\int_{x^*=0}^{-3}\frac{h_e(x)h^Q}{E(G(h,M,c))h_1{}^Q}dx^*}{\int_{x^*=0}^{-3}\frac{h^Q}{E(G(h,M,c))h_1{}^Q}dx^*}\right], \tag{48}$$

and

$$\frac{\partial f}{\partial h_m}=\frac{\partial}{\partial h_m}\left[6h_{m_0}{}^2\frac{h}{M^2}\left[\frac{Mh}{h_{m_0}}\coth\left(\frac{1}{2}\frac{Mh}{h_{m_0}}\right)-2\right]\right]. \tag{49}$$

The partial derivative of film force with respect to the squeezing velocity can be used to calculate the linear dynamic damping coefficient.

$$\begin{aligned}D&=-\left(\frac{\partial F}{\partial V}\right)\\ &=\frac{-\partial}{\partial V}\left[(-1)\left\{\left[-\left[6h_m-\frac{12}{\ln(\delta+1)}V\right]\int_{x^*=0}^{-3}\int_{x^*=0}^{x^*}\frac{h^Q}{E(G(h,M,c))h_1{}^Q}dx^*dx^*\right]\right\}\right]\\ &+c_1(h_m,V)\left[\int_{x^*=0}^{-3}\int_{x^*=0}^{x^*}\frac{h^Q}{E(G(h,M,c))h_1{}^Q}\frac{\partial f}{\partial h_m}dx^*dx^*\right].\end{aligned} \tag{50}$$

The following parameters values have been used in this article.

Physical Quantity	Symbol	Value of Physical Quantity
'Length of the bearing'	L	'$1.0\times10^{-1}m$'
'Inlet film thickness'	h_1	'$2.0\times10^{-4}m$'
'Outlet film thickness'	h_m	'$1.0\times10^{-4}m$'
'Profile parameter'	δ	'1.0'
Electrical conductivity	σ	h_0/m
'Lubricant viscosity Parameter'	Q	'$0\sim1$'
'Applied magnetic field'	B_0	$0, 0.95, 1.90 Wb/m^2$
'Roughness parameter'	c^*	'$(0, 0.4)\times10^{-4}m$'
'Steady minimum film thickness'	h_{m_0}	'$0.5\sim1.5$'
Hartmann number	M	$0\sim10$

3. Results and discussions

This study examines how surface roughness affects an exponential slider bearing's slider and dynamic properties when a magnetic field is present. These are affected by the roughness parameter, Hartmann number M, and profile parameter δ. Using the given values for the non-dimensional parameter in the current study yields the following outcomes.

- $c^*=0$, $l^* = 0$, Naduvinamani *et al.* [93] investigated the influence of magneto hydrodynamic coupling stresses on the dynamic properties of an exponential slider bearing (2017).
- Santhanakrishnan *et al.* [103] examined magneto hydrodynamics properties for wide porous slider bearings with an exponential film profile with $c^*=0$, Q (viscosity variation=0) (2016).

Squeeze Film Pressure

Fig. 2 illustrates the fluctuation of non-dimensional steady state pressure p^* with coordinate x^* for different Hartmann number and viscosity parameter Q values. An increase in the value of M leads to a noticeable rise in the non-dimensional p^* measure. As Hartmann number increases, the presence of the magnetic field enhances the overall pressure, leading to a more uniform pressure profile due to the damping effect of Lorentz forces. Conversely, increasing Q, which accounts for viscosity variation, results in a noticeable shift in pressure peaks and distribution while MHD forces can enhance pressure, viscosity variation can either counteract or amplify these effects depending on the flow conditions.

Fig. 3 shows the fluctuation of p^* with profile parameter δ for various values of Hartmann number M and steady minimum film thickness h_{m_0} with viscosity parameter $Q = 1$, roughness parameter $c^* = 0.4$ for both longitudinal and transverse roughness pattern for both longitudinal and transverse roughness patterns. The squeeze film pressure reduces as the viscosity variation parameter increases in both longitudinal and transverse roughness patterns.

For both longitudinal and transverse roughness, Fig. 4 illustrates the variation of p^* with h_{m_0} for varying values of M and Q. Moreover, p^* increases with increasing M in both scenarios for constant $\delta=1$. The results indicate that pressure increases with increasing M in both low and high viscosity variation scenarios. This is attributed to the strengthening of the Lorentz force, which enhances fluid resistance and contributes to higher pressure. Additionally, as Q increases, viscosity variation influences the pressure profile, leading to a reduction in peak pressure due to the weakening of lubricant viscosity. However, the MHD effect dominates at higher M, ensuring an overall pressure increase despite viscosity changes. This interplay suggests that optimizing M and Q can significantly influence the hydrodynamic performance of the porous slider bearing which is very useful in advancing the hydraulic systems used in mining equipment.

Fig. 5 illustrates the fluctuation in work load W^* as a function of h_{m_0} different viscosity parameters while maintaining a constant roughness parameterc^*. As Q increases, it is observed that it expands.

Fig. 6 illustrates non-dimensional work W^* with δ for various M and h_{m_0}. It is noted that the work increases as the Hartmann number M grows, as well as for both roughness patterns.

The steady state stiffness coefficient fluctuates with the profile parameter δ for different values of M, as seen in Fig. 7. As M

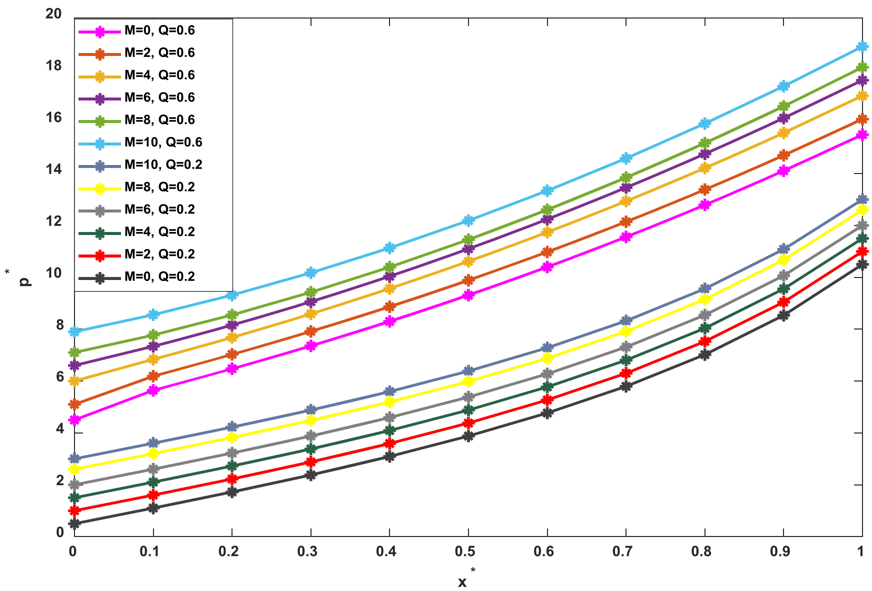

Fig. 2. MHD steady film pressure p^* as a function of x^* for different M and Q under $\delta = 1$ and $h_{m_0} = 1$.

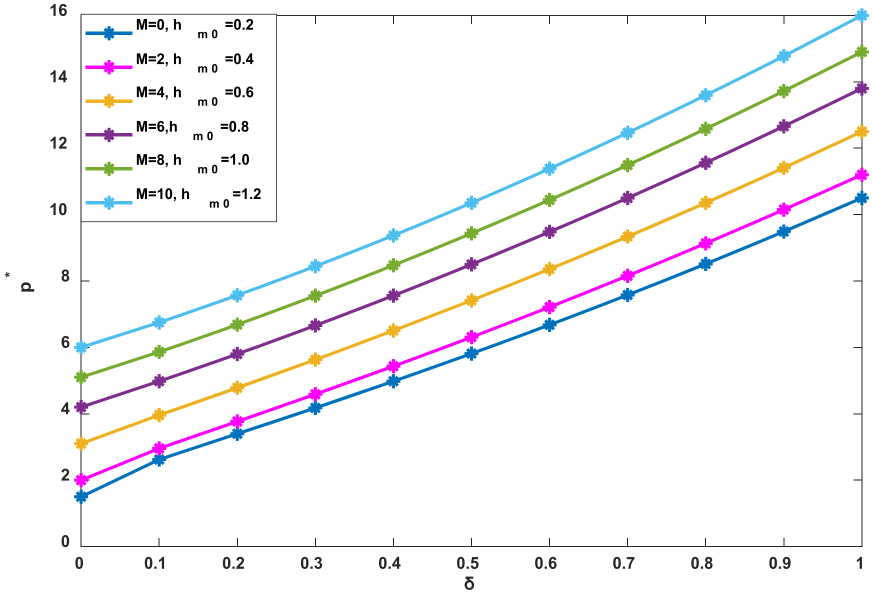

Fig. 3. Plot of MHD steady film pressure p^* as a function of δ for different M and h_{m_0} under $Q = 1$.

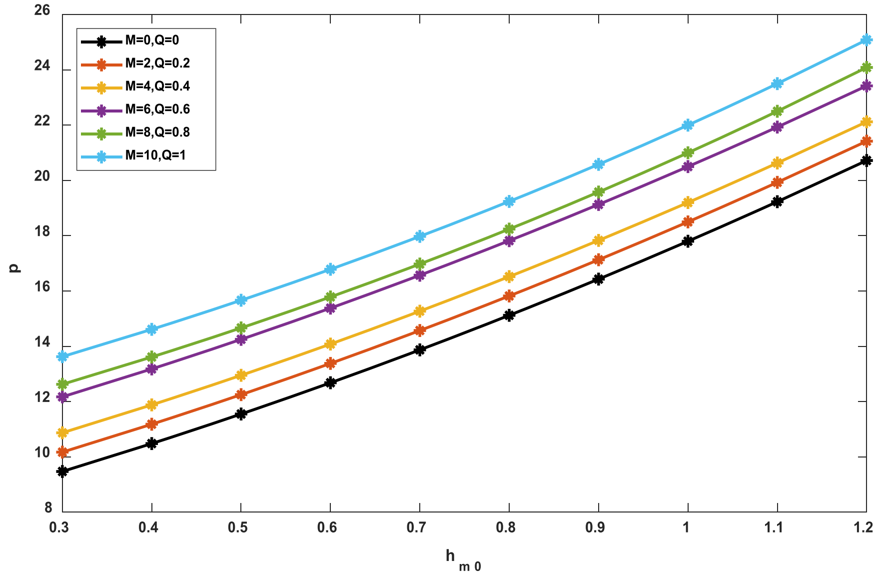

Fig. 4. Plot of MHD steady film pressure p^* as a function of h_{m_0} for different M and Q under $\delta = 1$.

increases, the transverse and longitudinal roughness patterns become more rigid. It is also demonstrated that the viscosity variation parameter increases the load carrying capacity.

Fig. 8 shows the variation of damping coefficient in a steady condition with profile parameter δ with $h_{m_0} = 1$ and $Q = 0.5$. With both types of roughness pattern, it is seen that D^* increases for increasing values of M and roughness parameter c^*. When compared to non-magnetic and Newtonian situations, the application of a magnetic field and the effect of the roughness parameter both enhance the value of the damping coefficient.

4. Conclusion

Based on the MHD thin-film lubrication theory, the MHD characteristic for a wide exponential-shaped porous rough slider bearing with an electrically conducting fluid in the presence of a transverse magnetic field is theoretically investigated. The following conclusion can be taken from the findings and discussions:

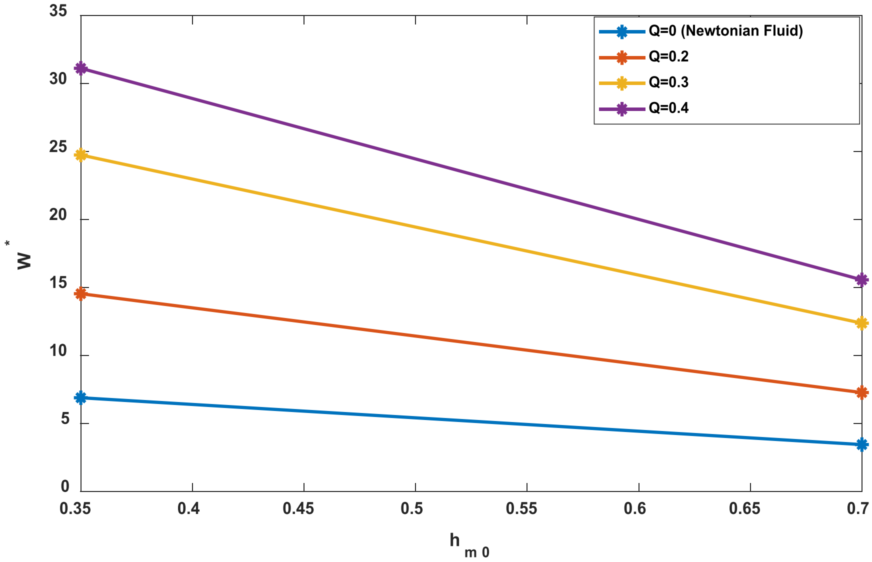

Fig. 5. Variation of non-dimensional work load W^* with h_{m_0} for different Q under $\delta = 1$.

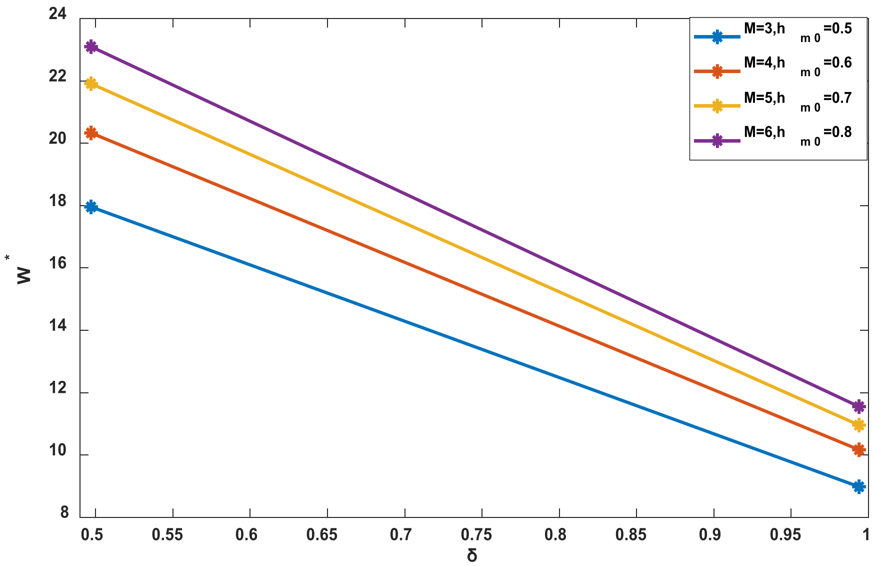

Fig. 6. Variation of non-dimensional work load W^* with δ for different M and h_{m_0} under $Q = 1$.

- The MHD dynamic Reynolds-type equation has been derived for the study of an MHD exponential-shaped porous slider bearing, taking into account the transient squeezing action.
- For the stable load carrying capacity, stiffness coefficient, and damping coefficient, a closed form solution is obtained.
- In contrast to the non-conducting lubricant (NCL) example, the effects of externally applied magnetic fields on the steady load and dynamic stiffness coefficients are more noticeable with greater values of the Hartmann number and the profile parameter and small values of the minimum film thickness.
- With higher Hartmann number and profile parameter values and lower minimum film thickness values, the effects of externally applied magnetic fields on the steady load and dynamic stiffness coefficients are increasingly noticeable.

The findings suggest that incorporating MHD effects enhances the load-carrying capacity and reduces frictional losses, making the system more efficient in high-performance and precision in engineering applications and mining industry. Additionally, the consideration of viscosity variation improves the accuracy of performance predictions, particularly in extreme temperature or pressure environments, ensuring better lubrication and durability. These insights can be effectively utilized in industries such as aerospace, automotive, mining, and manufacturing, where optimized bearing performance is crucial for reliability and energy efficiency.

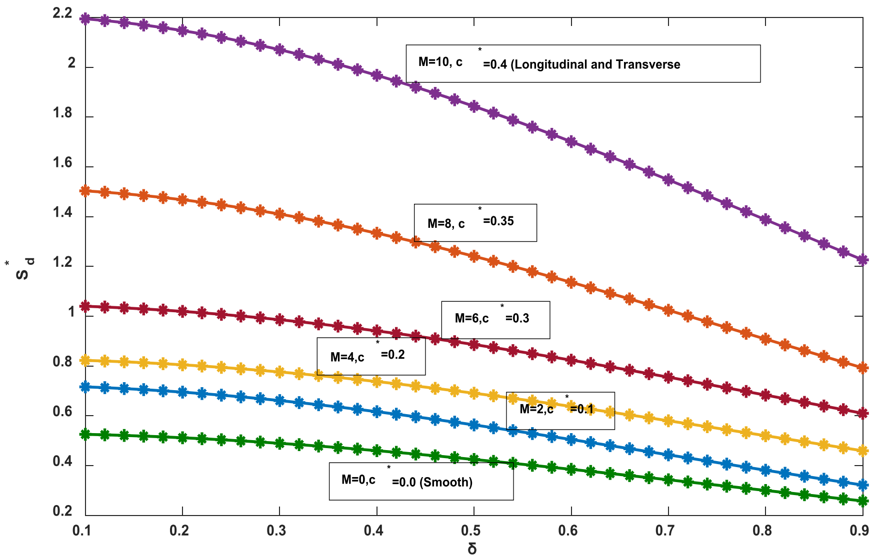

Fig. 7. Variation of non-dimensional dynamic stiffness coefficient S^* with δ for different M, c^* under $h_{m_0} = 1$.

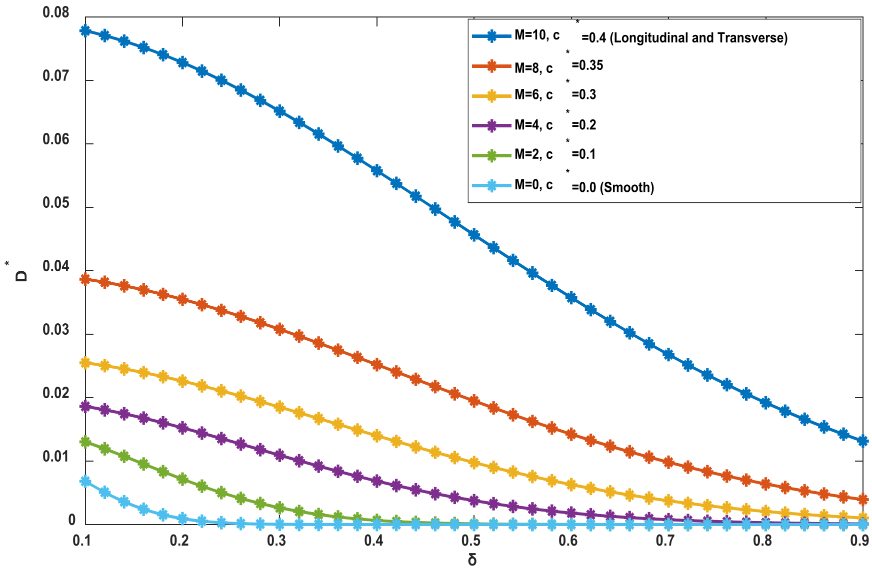

Fig. 8. Variation of non-dimensional dynamic damping coefficient D^* with δ for different M, c^* under $h_{m_0} = 1$.

Industrial Applications: Industries utilizing high-speed rotating equipment, such as mining industry, textile machinery and precision machining tools, rely on porous bearings for effective lubrication and minimal wear. The study's findings can improve lubricant distribution strategies, hydraulic systems in mining, and enhancing machine longevity. In applications where extreme temperature variations affect lubricant viscosity, such as aircraft landing gear mechanisms and automotive transmissions, understanding viscosity-dependent performance can optimize bearing efficiency under dynamic conditions.

CRediT authorship contribution statement

Zahoor Iqbal: Writing – original draft, Validation, Software, Methodology, Data curation, Conceptualization. **Nisha A.:** Writing – original draft, Validation, Software, Methodology, Conceptualization. **Vinoth kumar B.:** Writing – original draft, Software, Resources, Project administration, Methodology, Conceptualization. **Huiying Xu:** Visualization, Validation, Software, Resources, Project administration, Methodology, Data curation, Conceptualization. **Xinzhong Zhu:** Visualization, Validation, Supervision, Software, Resources, Project administration, Funding acquisition, Conceptualization. **Ridha Selmi:** Visualization, Software, Methodology, Funding acquisition. **Sahar Ahmed Idris:** Validation, Project administration, Methodology, Funding acquisition. **Ines Hilali**

Jaghdam: Writing – review & editing, Visualization, Validation, Software, Resources, Funding acquisition. **Ahmed M. Abed:** Visualization, Validation, Software, Resources, Project administration, Methodology, Funding acquisition.

Declaration of competing interest

The authors declare that they have no known competing financial interests or personal relationships that could have appeared to influence the work reported in this paper.

Acknowledgements

This work was supported by the National Natural Science Foundation of China (62376252); Key Project of Natural Science Foundation of Zhejiang Province (LZ22F030003); Zhejiang Province Leading Geese Plan (2025C02025, 2025C01056); Zhejiang Province-Land Synergy Program (2025SDXT004–3). The authors extend their appreciation to Deanship of Research and Graduate Studies at King Khalid University for funding this work through Large Research Project under grant number R.G.P.2/470/45. This work was supported in part by Prince Sattam bin Abdulaziz University (PSAU) funding programme project number (PSAU-2025/R/1446). This work is supported by Princess Nourah bint Abdulrahman University Researchers Supporting Project number (PNURSP2025R845), Princess Nourah bint Abdulrahman University, Riyadh, Saudi Arabia. The authors extend their appreciation to the Deanship of Scientific Research at Northern Border University, Arar, KSA for funding this research work through project number NBU-FFMRA-2025–2714–01.

Data availability statement

There is no associated data included in this article.

References

[1] J. Bernard, Hamerock, fundamentals of fluid film lubriaction, NASA Ref. Public. 1255 (1991).
[2] J. Jaya Chandra Reddy, C. Eswara Reddy, K. Rama Krishna Prasad, Effect of viscosity variation on the squeeze film performance of a narrow hydrodynamic journal bearing operating with couple stress fluids, Proc. I MechE Part J 222 (2016) 141–151.
[3] Hanumagowda Bannihalli Naganagowda, Effect of magneto hydrodynamic and couple stress on steady and dynamic characteristics of plane slider bearing, Tribol. Online 11 (2016) 40–49.
[4] N.B. Naduvinamani, S.T. Fathima, B.N. Hanumagowda, Magneto hydrodynamic couple stress squeeze film lubrication of circular stepped plates, Proc. Institut. Mech. Eng., Part J 225 (2011) 111–119.
[5] J.R. Lin, Dynamic characteristics for wide magneto hydrodynamic slider bearings with a power law film profile, Appl. Math. Modell. 36 (2012) 4521–4528.
[6] N.B. Naduvinamani, A. Siddangouda, P. Siddaram, Effect of magneto hydrodynamic couple stresses on dynamic characteristics of exponential slider bearing, Tribol. Industry 39 (2012) 31–44.
[7] S. Kesavan, A. Chamkha, S.Krishnan Narayanan, Magneto hydrodynamic squeeze film characteristics between finite porous parallel rectangular plates with surface roughness, Int. J. Numer. Method. Heat Fluid Flow 2 (2014) 1595–1609.
[8] R.B. Kudenatti, N. Muralidhara, H.P. Patil, Numerical solution of the MHD Reynolds equation for squeeze film lubrication between porous and rough rectangular plates, Tribology (2013) 1–10.
[9] N.M. Bujurke, N.B. Naduvinamani, D.P. Basti, Effect of surface roughness on MHD squeeze film characteristics between finite rectangular plates, Tribol. Int. 7 (2011) 916–921.
[10] H. Christensen, Stochastic models for hydrodynamic lubrication of rough surfaces, Proc. Institut. Mechan. Eng. 1 (1969) 1013–1026.
[11] B.N. Hanumagowda, Thippeswamy Gonchigara, J. Santhosh Kumar, H.M Shiva Kumar, Study of effect of magneto hydrodynamic and couple stress on steady and dynamic characteristics of porous exponential slider bearing, J. Phys. 1000 (2018).
[12] J.R. Lin, C.R. Hung, Analysis of dynamic characteristics for wide slider bearings with an exponential film profile, J. Mar. Sci. Technol. 12 (2004) 217–221.
[13] N.B. Naduvinamani, K. Archana, Effect of viscosity variation on the micropolar fluid squeeze film lubrication of a short journal bearing, Adv. Tribol. (2013) 1–7.
[14] Biradar Kashinath, Hanumagowda, Nagangowda Bannihalli, MHD effect on porous wide composite slider bearing lubricated with a couple stress fluid, Tribol. Online 10 (2015) 11–20.
[15] C.K. Sreekala, Syeda Tasneem Fathima, B.N. Hanumagowda, Stochastic Reynolds equation for porous slider bearing having exponential and secant film profile lubricated with couple stress fluids in the presence of transverse magnetic field, Int. J. Pure Appl. Math. 113 (2017) 343–351.